Appendix S1

MATERIAL AND METHODS

Real-time PCR for melanogenesis gene transcripts

Gene expression analysis was carried out using the ABI Prism 7000 real-time PCR system (Applied Biosystems, Foster City, CA). Reactions (10 µl) were carried out in replicates using TaqMan universal PCR master mix (Applied Biosystems) and FAM- and TAMRA-labeled TaqMan probes. normalization was carried out using 18S rRNA probes labeled with VIC and MGB 4319413E-0710034. Data analysis was carried out as previously described (1).

Transmission electron microscopy

Transmission electron microscopy was performed on hyper- and hypo-pigmented lesions using standard protocols. Briefly, 3mm biopsies were fixed in 2.5% gluteraldehyde and 4% paraformaldehyde, osmicated in 1 % osmium tetroxide, dehydrated in graded series of alcohol and infiltrated with Epon 812 resin. Ultrathin sections were cut on RMC ultramicrotome, collected on copper grids and stained with uranyl acetate and lead citrate. Samples were visualized on Tecnai G2 20 twin (FEI) transmission electron microscope.

1. Natarajan VT, Singh A, Kumar AA et al (2010). Transcriptional upregulation of Nrf2-dependent phase II detoxification genes in the involved epidermis of vitiligo vulgaris. J Invest Dermatol; 130(12): 2781-2789.

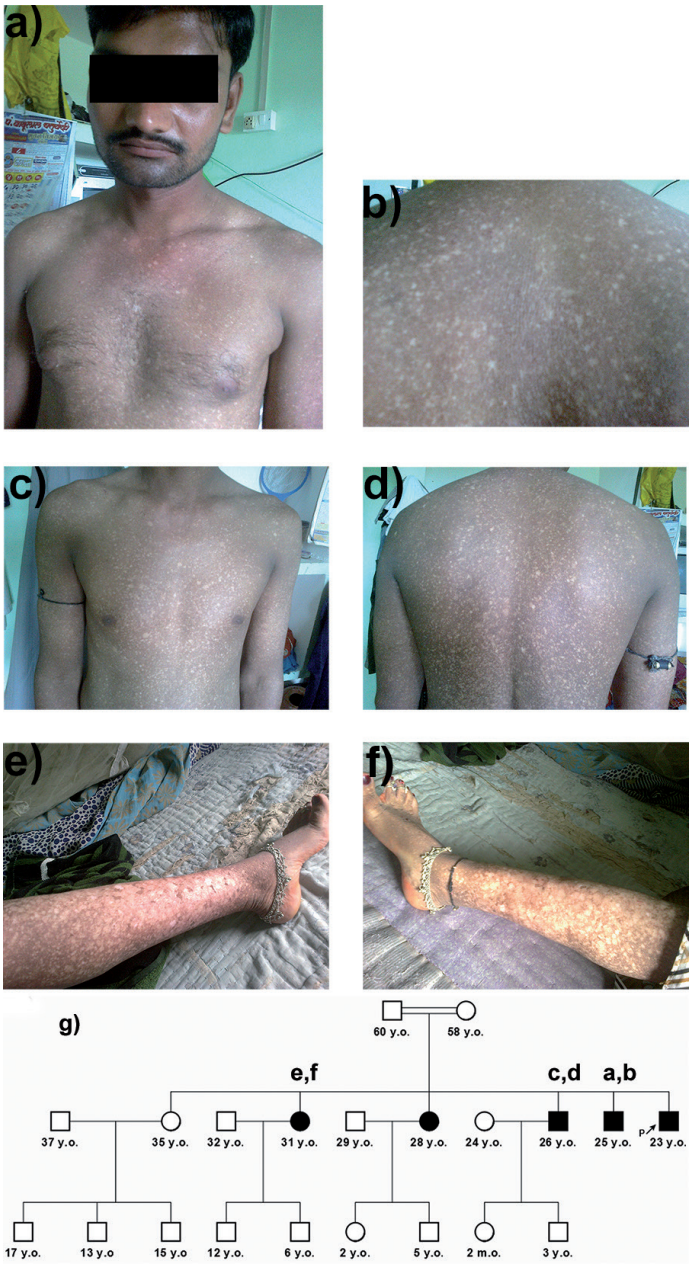

Fig. S1. Mottled hyper- and hypopigmented macules in 3 family members of the proband. (a, b) Innumerable mottled hypo- and hyperpigmented macules involving 1) chest, 2) back in the 25-year-old brother, labelled as a,b in the pedigree chart in Fig. g. (c, d) Multiple mottled hyper- and hypopigmented macules and patches involving 1) chest, abdomen and 2) back in the 26-year-old brother, labelled as c,d in the pedigree chart in Fig. g. (e, f) Multiple irregular hypopigmented patches involving the legs and relatively sparing the dorsa of feet in the eldest sister, labelled as e,f in the pedigree chart in Fig. g.

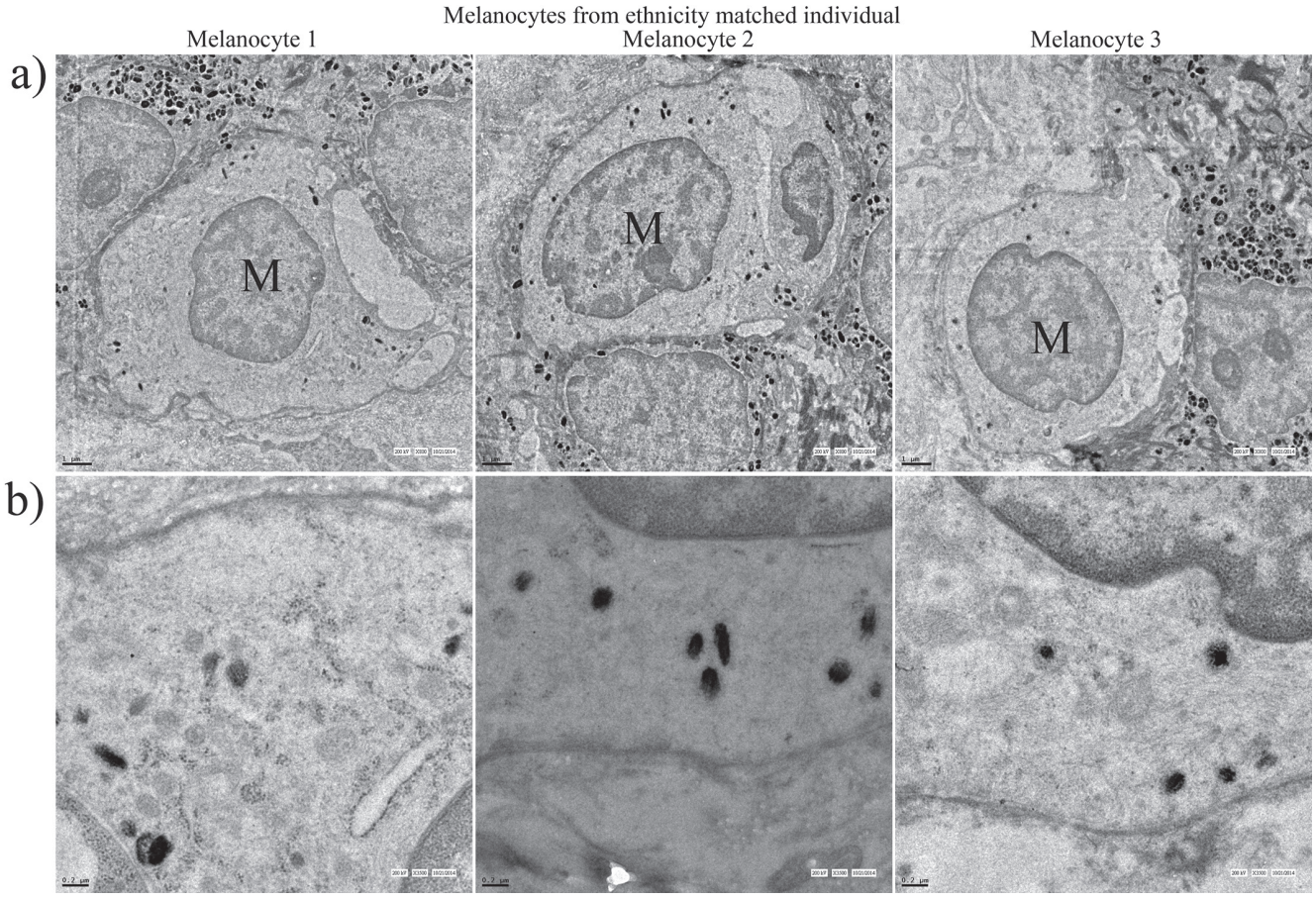

Fig. S2. Ultrastructural details of melanocytes in ethnicity-matched normal skin: Three representative micrographs of melanocytes (M, at the dermal–epidermal junction) containing melanosomes in the ethnicity matched normal skin (vertical panel 1, 2 and 3). Horizontal panel a) shows the melanocytes at dermal–epidermal junction at low magnification (scale bar 1 μm). Horizontal panel b) shows magnified view of the melanocytes (scale bar 0.2 μm).

The authors are thankful to the transmission electron microscopy (TEM) facility at CSIR – Institute of Genomics and Integrative Biology. The authors acknowledge Dr. Rajesh S. Gokhale, CSIR-IGIB, for suggestions. The authors thank Mahendra Pratap Singh for his help in acguiring TEM micrographs. *Funding source:* This work is supported by program support grant by Council of Scientific and Industrial Research, India (BSC0302) and INSPIRE faculty grant (IFA12-LSBM-35) from Department of Science and Technology, India.

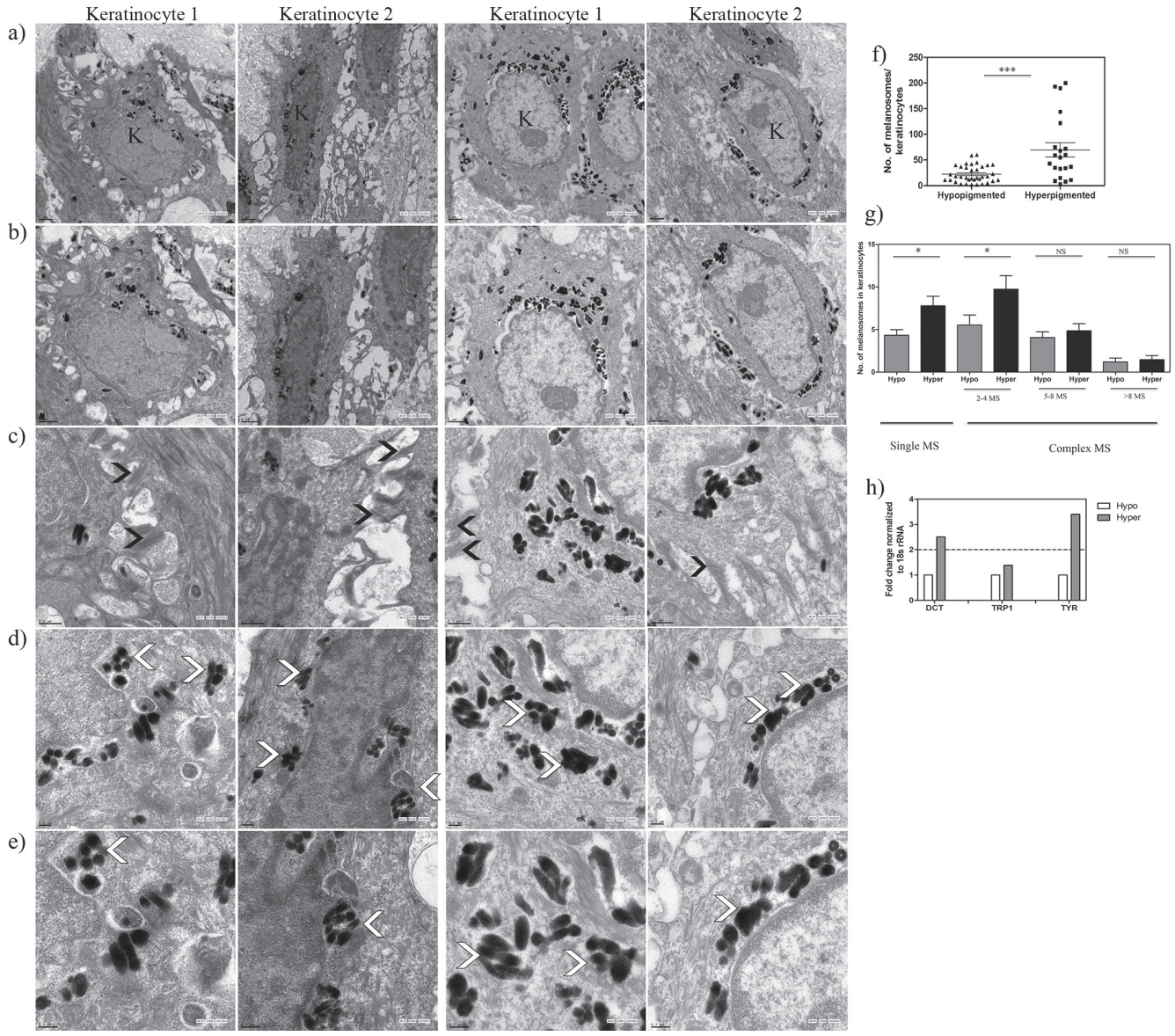

Fig. S3. Altered melanosome numbers in keratinocytes of hypopigmented vs hyperpigmented lesions: Presence of melanosomes in 2 representative keratinocytes (K) in hypopigmented (vertical panel 1 and 2) and hyperpigmented lesion (vertical panel 3 and 4). Micrographs in a) and b) horizontal panels show keratinocytes at lower magnifications (scale bar 1 μm). Horizontal panel c) shows presence of prominent desmosomal connections in cell-cell junction (black arrowheads) between neighbouring keratinocytes (scale bar 0.5 μm). Magnified images in d) and e) reveal presence of melanosomes in clusters (white arrowheads) in keratinocytes of both hypo- and hyperpigmented lesions (scale bar 0.2 μm). f) Number of melanosomes in keratinocytes of hypo- and hyperpigmented skin plotted as column bar graph. Keratinocytes in hyperpigmented epidermis show significantly higher number of melanosomes per keratinocytes compared to hypopigmented skin ($n = 36$ keratinocytes counted in hypopigmented, $n = 21$ keratinocytes counted in hyperpigmented skin). *** indicates p-value < 0.0001 using unpaired t test. g) Distribution pattern of melanosomes in keratinocytes plotted as present as single, and in clusters of 2–4, 5–8 and greater than 8 ($n = 15$ each for hypo- and hyperpigmented skin). The melanosome numbers are significantly lower in hypopigmented skin in both single as well as in 2–4 clusters. * indicates p-value < 0.05 using unpaired t test. There was no significant difference in number of melanosomes in clusters of 5–8 and >8 melanosomes per cluster. h) Real-time PCR analyses of DCT, TRP1 and TRP2 carried out using Taqman duplex assays were normalised to 18S ribosomal RNA (rRNA) and represented as fold change with respect to corresponding hypopigmented lesion plotted in a bar graph. Fold change was calculated using $2^{-\Delta\Delta Ct}$, where $\Delta\Delta Ct$ represents ΔCt of hyperpigmented–ΔCt of hypopigmented skin. DCT- Dopachrome tautomerase, TRP1-Tyrosinase related protein 1, TYR- Tyrosinase. Horizontal line represents fold change greater than 2-fold.

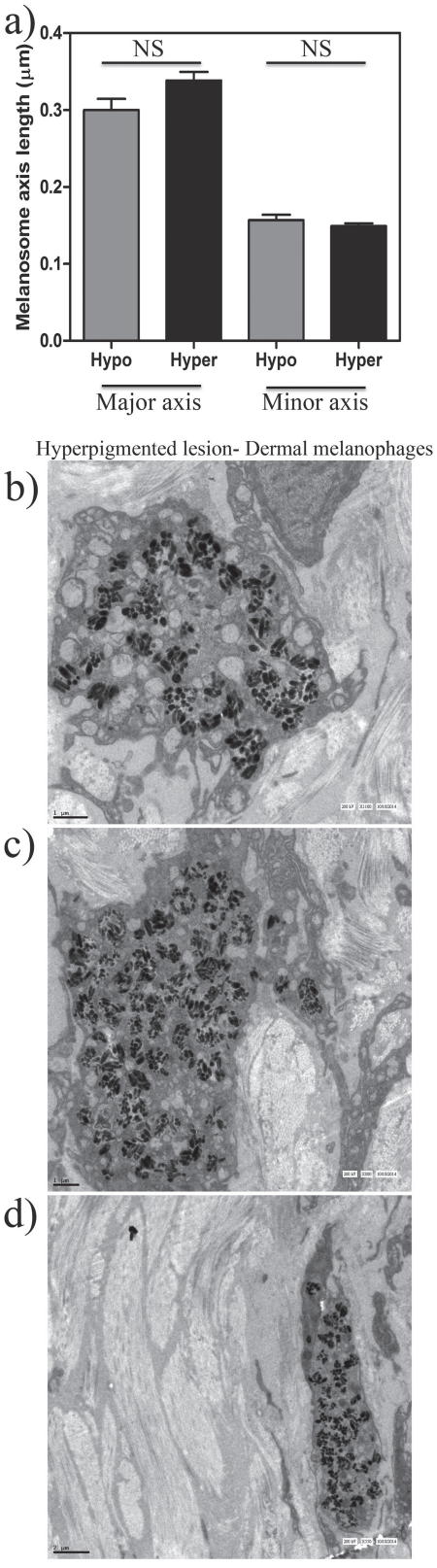

Fig. S4. Melanosome size in keratinocytes and dermal melanophages in dyschromatoses universalis hereditaria: a) length of major and minor axis of melanosomes in keratinocytes of hypo- and hyperpigmented skin plotted as column bar graph ($n = 11$ each). There was no significant difference in the melanosome sizes in the 2 lesion types (p-value NS or not significant using unpaired t-test). b) Three representative micrographs showing melanophages in the dermis of hyperpigmented lesion.